Am J Cancer Res 2022;12(5):2363-2375
www.ajcr.us /ISSN:2156-6976/ajcr0142534

Original Article

PD-L1 deficiency sensitizes tumor cells to DNA-PK inhibition and enhances cGAS-STING activation

Zhen Xue[1,2*], Shuang Zheng[1,2*], Dongli Linghu[1], Boning Liu[1], Yi Yang[3], Mei-Kuang Chen[4], Hua Huang[1], Jiaming Song[1], Hongyue Li[5], Jing Wang[1], Mien-Chie Hung[4,6], Diansheng Zhong[1,2], Linlin Sun[1]

[1]Tianjin Key Laboratory of Lung Cancer Metastasis and Tumor Microenvironment, Lung Cancer Institute, Tianjin Medical University General Hospital, Tianjin 300052, P. R. China; [2]Department of Medical Oncology, Tianjin Medical University General Hospital, Tianjin 300052, P. R. China; [3]Institute of Pathology and Southwest Cancer Center, Southwest Hospital, Third Military Medical University, Chongqing 400038, P. R. China; [4]Department of Molecular and Cellular Oncology, The University of Texas M. D. Anderson Cancer Center, Houston, Texas 77030, USA; [5]Tianjin General Surgery Institute, Tianjin Medical University General Hospital, Tianjin 300052, P. R. China; [6]Graduate Institute of Biomedical Sciences and Center for Molecular Medicine, China Medical University, Taichung, Taiwan. [*]Equal contributors.

Received February 24, 2022; Accepted May 2, 2022; Epub May 15, 2022; Published May 30, 2022

Abstract: Immunotherapies that block PD-L1/PD-1 immune checkpoint proteins represent a landmark breakthrough in cancer treatment. Although the role of PD-L1 in suppressing T cell activity has been extensively studied, its cancer cell-intrinsic functions are not well understood. Herein, we demonstrated that PD-L1 is important for the repair of DNA damage in cancer cells. Mechanically, depletion of PD-L1 led to the downregulation of the critical molecules involved in the homologous recombination (HR) repair pathway, such as ATM and BRCA1, but did not obviously affect the non-homologous end joining (NHEJ) pathway. Notably, PD-L1 silence sensitized cancer cells to chemotherapy agents and the inhibitor of DNA-PK, which is an important kinase for NHEJ. Furthermore, PD-L1 depletion potentiated DNA damage-induced cGAS-STING pathway and induction of IFNβ. The regulation of DNA repair and cGAS-STING pathway by PD-L1 represents its connection with innate immunity that can be exploited to enhance the efficacy of existing immunotherapy. Our findings thus expand the focus of PD-L1 from tumor antigen-specific CD8+ T cells to innate immunity, and support targeting tumor-intrinsic PD-L1 combined with DNA-PK inhibition for tumor eradication, through promoting synthetic lethality and innate immune response.

Keywords: Immune checkpoint, DNA damage response, homologous recombination, non-homologous end joining, synthetic lethality, innate immunity

Introduction

Genomic instability is one of the hallmarks of cancer [1]. DNA damage response (DDR), which involves a complex network of proteins acting to cope with damaged DNA, is essential for the maintenance of genomic integrity. Deficiency in certain high fidelity DDR machineries, such as homologous recombination (HR), will lead to higher dependence on the compensatory non-homologous end-joining (NHEJ), which is likely error-prone [2-4]. DDR signaling events are largely coordinated by three key apical kinases: Ataxia telangiectasia mutated (ATM), ATM- and RAD3-related (ATR), and DNA-dependent protein (DNA-PK). ATM plays an important role in HR, ATR is crucial for maintaining replication fork stability, and DNA-PK is critical for NHEJ [5, 6]. Defects in DDR provide opportunities for utilizing the concept of synthetic lethality to develop new cancer treatment modalities [7]. Several DDR inhibitors targeting ATM, ATR and DNA-PK have been evaluated in clinical trials [8]. Biomarkers of responsiveness to DNA-PK inhibition remain unclear, and further identification of exploitable defects is needed to improve the efficacy of the DDR inhibitor.

DDR deficiency has been linked with the activation of anti-tumor immunity primarily via promoting innate immune response, which is initially characterized as the first host line to

defense against pathogens [9]. Cytosolic damaged DNA caused by DDR gene inactivation or DNA-damaging treatments can be recognized by the nucleic acid sensor cyclic GMP-AMP (cGAMP) synthase (cGAS). Upon binding of cytosolic DNA, cGAS promotes the synthesis of cGAMP that bind to and activate the endoplasmic reticulum-anchored stimulator of interferon gene (STING), which then recruits and activates TANK-binding kinase 1 (TBK-1) and heterodimeric IKKα/β kinase. These kinases in turn activate interferon regulatory factor 3 (IRF3) and nuclear factor-κB (NF-κB), leading to the release of type I interferon (IFNs) IFN-α and IFN-β. IFNs bind to the heterodimeric IFN receptor and activate Janus kinase 1 (JAK1)-the signal transducer and activator of transcription (STAT) signaling, ultimately inducing the expression of IFN-stimulated genes and promoting the mobilization of CD8+ T cells for tumor eradication [10]. As agonists of cGAS-STING pathway, DNA damage-inducing therapies have been shown to act synergistically with anti-PD-1/PD-L1 immunotherapy to inhibit tumor growth [11]. A more comprehensive understanding of the DNA-damage-induced innate immune responses is essential to further improve the efficacy of current cancer therapies.

PD-L1 is a key immune checkpoint protein that binds to PD-1 on T cells and suppress T cell activity [12]. Immunotherapies that block PD-1/PD-L1 binding have achieved promising clinical outcomes in multiple cancer types. Interestingly, increasing evidence indicates that PD-L1 is also involved in a variety of PD-1-independent functions in cancer cells [13-18], including its crosstalk with DNA damage repair. PD-L1 expression can be significantly induced by conventional DNA damaging-agents such as radiotherapy and chemotherapy, in an ATR-dependent manner [19-21]. Moreover, knockdown of PD-L1 has been shown to sensitize cancer cells to ionizing radiation (IR) [16]. These findings suggest that PD-L1 is potentially involved in the process of DDR. However, the specific function of PD-L1 in regulating DDR needs to be further clarified.

In this study, we sought to investigate the role of PD-L1 in DNA damage repair and cGAS-STING mediated innate immunity, aiming to broaden the understanding of PD-L1 biological functions and provide the rationale for targeting tumor-intrinsic PD-L1 for cancer treatment.

Materials and methods

Cell lines, compounds, and antibodies

The MDA-MB-231 and BT549 triple-negative human breast cancer cell lines and A549 lung cancer cell line were obtained from the American Type Culture Collection (ATCC, Manassas, VA, USA). The cells were cultured in RPMI-1640 or DMEM medium (Thermo Fisher Scientific, Waltham, MA, USA) supplemented with 10% fetal bovine serum (Thermo Fisher Scientific) at 37°C in a humidified atmosphere with 5% CO_2. NU7441, PI-103, VE-822, and KU60019, Olaparib, cisplatin, etoposide were obtained from Selleck (Houston, TX, USA). The comet assay reagent kit (Catalog # 4250-050-K) was obtained from Trevigen (Gaithersburg, MD, USA). ATM, p-ATM (S1981), ATR, p-ATR (Thr1989), DNA-PK, p-DNA-PK (S2056), p-STAT1 (Tyr701), p-STING (Ser365), p-TBK1 (Ser172), p-IRF3 (Ser386), Caspase-3, PARP, cleaved PARP, cGAS, γH2AX (Ser139) and β-actin antibodies were purchased from Cell Signaling Technology (Cambridge, MA, USA).

Generation of stable cells by lentiviral infection

To generate PD-L1 stable knockdown or PD-L1 over-expression (OE) cells, 293T cells were co-transfected with shPD-L1 or PD-L1 over-expression constructs (4 μg) with pCMV-dR8.2 (3 μg) and pCMV-VSVG (1 μg) helper constructs using Lipofectamine 2000 reagent (Life Technologies, Carlsbad, CA, USA). Viral stocks were harvested from the culture medium after 2 days and then filtered to remove non-adherent 293T cells. To select cells that stably express PD-L1 shRNA or OE constructs, cells were plated at sub-confluent densities and infected with a cocktail of 1 ml of virus-containing medium, 1 ml of regular medium and 8 μg/ml polybrene, and then selected in 1 μg/ml of puromycin (InvivoGen, San Diego, CA, USA) 48 hours after lentivirus infection.

Cell proliferation assay

Cell viability was determined using a Cell Counting Kit-8 (CCK8) assay (Bimake.cn, Shanghai, China). Cells (4×10^3 cells/100 μL/well) were seeded in 96-well plates and then subjected to drug treatments for 48 h. After drug exposure, 10 μL of CCK8 reagent was added to each well, and the cells were cultivat-

ed at 37°C for 1.5 h with 5% CO_2. The absorbance at 450 nm was measured with a microplate reader (Beckman Coulter, Brea, CA, USA). The half-maximal inhibitory concentration (IC50) values were calculated using GraphPad Prism.

Alkaline comet assay

Alkaline comet assay was performed using a comet assay reagent kit according to the manufacturer's instructions. Briefly, after drug treatment, cells were collected and mixed gently with LM agarose, and added onto comet slides. The slides were then placed at 4°C in the dark for 10 min and immersed in lysis solution for 1 h at 4°C. After that, the slides were immersed in freshly prepared alkaline unwinding solution for 20 min at room temperature and subsequently electrophoresed under alkaline conditions. The slides were then fixed with 70% ethanol, stained with SYBR Gold staining solution, and visualized with a fluorescence microscope.

Western blotting analysis

Cells were collected and lysed on ice in RIPA lysis buffer containing protease and phosphatase inhibitors (Med Chem Ex-press, Shanghai, China). The samples were centrifuged at 15,000 r/min for 15 min at 4°C. Protein aliquots of 25 μg were loaded for SDS-polyacrylamide gel electrophoresis, transferred to a PVDF membrane (Bio-Rad, Hercules, CA, USA), and then blocked with 5% nonfat milk or 5% bovine serum albumin at room temperature for 1 h. The membrane was then incubated with primary antibodies at 4°C overnight and then with an HRP-conjugated species-specific secondary antibody (ZSGB-BIO, Beijing, China) at room temperature for 1 h. The immunoreactive bands were visualized using Immobilon Western HRP Substrate (Millipore, Billerica, MA, USA).

Immunofluorescence microscopy

Cells were fixed in 4% paraformaldehyde at room temperature for 20 minutes and blocked with 5% BSA for 1 h. The cells were then incubated with primary antibodies overnight at 4°C, washed with PBS, and further incubated with a fluorochrome-conjugated secondary antibody for 1 h at room temperature in the dark. The nuclei were stained with 4',6-diamidino-2-phenylindole (DAPI) contained in the mounting reagent. Fluorescence images were captured using an Olympus microscope.

Real-time PCR

Total RNA was isolated using Trizol reagent (Invitrogen, Carlsbad, CA, USA). The first-strand cDNA was prepared using the Prime Script 1st strand cDNA Synthesis Kit (Vazyme, Nanjing, China) according to the manufacture's protocol with 1 μg of total RNA. All RT-PCR reactions were performed in a 20-μl mixture containing 1×SYBR Green Master Mix (Vazyme Biotech Co., Ltd China), 0.2 μmol/L of each primer, and 2 μl of cDNA template. Primers used are shown in Table S1. Real-time PCR was performed using the Applied Biosystem 7900 system (USA) under the following cycling conditions: (step 1) 95°C for 3 min, (step 2) 40 cycles of 95°C for 10 sec, and 60°C for 30 sec, followed by the melting curve stage. The relative PD-L1, ATM, ATR, DNA-PK and BRCA1 expression levels were normalized to that of GAPDH.

Crystal violet staining

Cells were seeded in a 24-well plate and incubated for 18-24 h to enable adhesion to wells. The cells were then subjected to drug treatment for 48 h. After that, the cells were fixed with 4% paraformaldehyde (500 μL/well) at room temperature for 0.5 h, stained with 0.5% crystal violet staining solution (500 μL/well) at room temperature for 30 min, and then washed three times with deionized water.

Flow cytometry analysis of apoptosis

7-AAD was used to evaluate apoptosis. Briefly, cells were treated with drugs for 48 h and then collected and stained with 7-AAD for 15 min in the dark. The cells were analyzed by flow cytometry (BD Biosciences) within 1 h. The data were analyzed with FlowJo software.

Gene correlations analysis

The correlations between PD-L1 and DDR-associated genes ATM, ATR and DNA-PK in breast cancer (BRCA) and TNBC were analyzed on TIMER 2.0 (http://timer.cistrome.org/). Correlations were calculated by using Spearman's correlation coefficient (rho). The breast

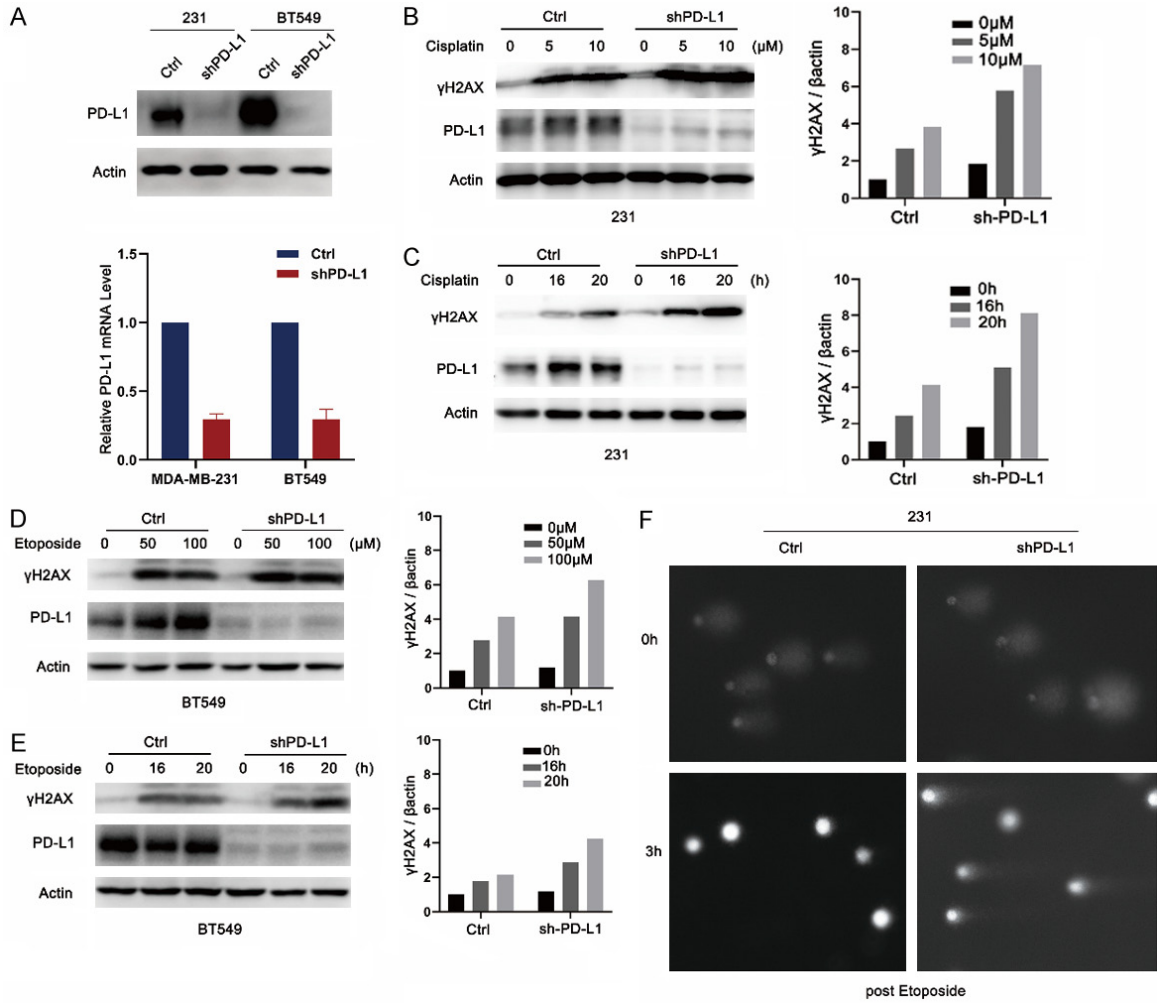

Figure 1. PD-L1 depleted cancer cells show deficiency in DNA damage repair. A. Western blot and qRT-PCR analysis of PD-L1 expression in MDA-MB-231 and BT549 cell lines with or without PD-L1 KD. B. Western blot analysis of γH2AX in MDA-MB-231 cells with or without PD-L1 KD treated with cisplatin at the indicated doses for 20 h. C. Western blot analysis of γH2AX in MDA-MB-231 cells with or without PD-L1 KD treated with 5 μM cisplatin at the indicated time points. D. Western blot analysis of γH2AX in BT549 cells with or without PD-L1 KD treated with etoposide at the indicated doses for 20 h. E. Western blot analysis of γH2AX in BT549 cells with or without PD-L1 KD treated with 50 μM etoposide at the indicated time points. F. Analysis of DNA comet tails by alkaline comet assay in MDA-MB-231 cells with or without PD-L1 KD treated with 50 μM etoposide for 20 h and then released from etoposide for 0 h and 3 h to allow DNA repair.

cancer (BRCA) gene expression data were obtained from The Cancer Genome Atlas (TCGA) database, 1104 samples were divided into two groups according to the expression level of PD-L1, and the expression of ATM, ATR and DNA-PK in each group was calculated.

Statistical analysis

Statistical analyses were performed using GraphPad Prism 8.0 software. All data are presented as the mean ± standard deviation (SD). Unpaired two-tailed t tests were used for comparisons between two groups. $P < 0.05$ was considered to indicated statistical significance. (*$P < 0.05$, **$P < 0.01$, ***$P < 0.001$).

Results

PD-L1 is essential for DNA damage repair

To investigate the function of PD-L1 in DNA damage repair, we generated PD-L1 stable knockdown (KD) MDA-MB-231 and BT549 triple-negative breast cancer (TNBC) cells and verified the KD efficiency by western blot and qRT-PCR. As shown in **Figure 1A**, the levels of PD-L1 protein (upper panel) and mRNA (lower

panel) were significantly inhibited in PD-L1 KD cells. Next, we treated these cells with cisplatin or etoposide, two conventional DNA-damaging agents, as indicated doses and time, and evaluated the levels of rH2AX, a well-established marker for DNA damage. We found that, compared with PD-L1 WT cells, PD-L1 KD cells exhibited significantly higher rH2AX levels in response to DNA damage induced by cisplatin or etoposide (**Figures 1B-E**, S1A and S1B). Similar results were found by immunofluorescence analysis (Figure S1C and S1D). We speculated that the enhanced DNA damage might result from the alteration of DNA repair capacity. To test the hypothesis, we used a comet assay to evaluate their DNA repair capacity after recovery from the treatment of etoposide. The "comet head" represents undamaged DNA, whereas the extension of the "comet tail" reflects the extent of DNA breaks in a particular cell. As shown in **Figure 1F**, after 3-hour recovery from etoposide treatment for 20 h, DNA damage was well repaired in PD-L1 WT cells, in contrast, obvious comet tails were still observed in PD-L1 KD cells, suggesting that PD-1 depletion leads to deficiency in DNA damage repair. Together, these results indicate that PD-L1 is essential for the repair of DNA damage.

PD-L1 depletion leads to decreased expression and activation of ATM and ATR

To investigate the underlying molecular mechanisms, we evaluated the expression of DDR-related genes in these cells. As shown in **Figure 2A**, we found that both the mRNA (left panel) and protein (right panel) levels of ATM, one of the major kinases in HR pathway, were dramatically decreased in PD-L1 KD cells, suggesting that PD-L1 is important for the expression of ATM. The expression of BRCA1, another key protein mediating HR, was also significantly lowered in PD-L1 KD cells (**Figure 2B**). Similarly, the expression of ATR, the major kinase in response to the replication stress, was also down-regulated in PD-L1 KD cells (**Figure 2C**). In contrast, the level of DNA-PK, a crucial kinase for NHEJ, was not obviously altered upon PD-L1 depletion (**Figure 2D**). These results suggest that PD-L1 is important for the expression of core proteins in HR pathways, such as ATM and BRCA1. The initiation of DNA repair relies on the phosphorylation and activation of ATM, ATR or DNA-PK. The altered expression of these key DDR kinases prompted us to investigate whether their activation status in response to DNA damage was affected. Next, we treated the cells with etoposide and evaluated the phosphorylation of these kinases. Consistently, the phosphorylation levels of ATM (p-ATM S1981) and ATR (p-ATR Thr1989) induced by etoposide were significantly decreased in PD-L1 KD cells (**Figure 2E** and **2F**). In contrast, the phosphorylation of DNA-PK (p-DNA-PK S2056) was not obviously affected by PD-L1 depletion (**Figure 2G**). These results demonstrate that PD-L1 depletion leads to downregulation of ATM and ATR expression and attenuates their activation in response to DNA damage, but does not have an obvious effect on DNA-PK.

ATM expression is significant positively correlated with PD-L1 expression in cancer patients

To validate the clinical relevance of the results, we used the TIMER 2.0 database to calculate the correlation of PD-L1 expression with ATM, ATR or DNA-PK, in two subsets of breast cancer patients, BRCA and TNBC. The Spearman's correlation coefficient (rho) was shown with the associated *p* value. We found that the expression of each of the three DDR kinases was positively correlated with PD-L1 (**Figure 3A**). Notably, ATM and ATR showed significant positive correlation with PD-L1, with rho values of 0.508 and 0.426 ($P < 0.01$) in BRCA dataset, and 0.518 and 0.519 ($P < 0.01$) in TNBC dataset, respectively (**Figure 3A**, left and middle panels), while DNA-PK showed less significant correlation, with rho values of 0.325 ($P < 0.01$) in BRCA dataset and 0.31 ($P < 0.01$) in TNBC dataset (**Figure 3A**, right panel). To further validate the findings, we evaluated the expression of these DDR kinases in cancer patients with high or low PD-L1 expression using TCGA BRCA sample data (**Figures 3B-D**, S2A-C). Compared with the PD-L1 low-patients, the patients with PD-L1 high expression showed higher expression of ATM ($P < 0.01$) (**Figure 3B**), but not of ATR ($P < 0.01$) (**Figure 3C**) or DNA-PK ($P=0.034$) (**Figure 3D**). These results suggest that ATM, a critical kinase for HR pathway, is significantly positively correlated with PD-L1 in cancer patients.

PD-L1 depletion sensitizes cancer cells to DNA-PK inhibition and chemotherapy agents

Based on the findings that ATM expression was lowered in PD-L1 depleted cells, we speculated

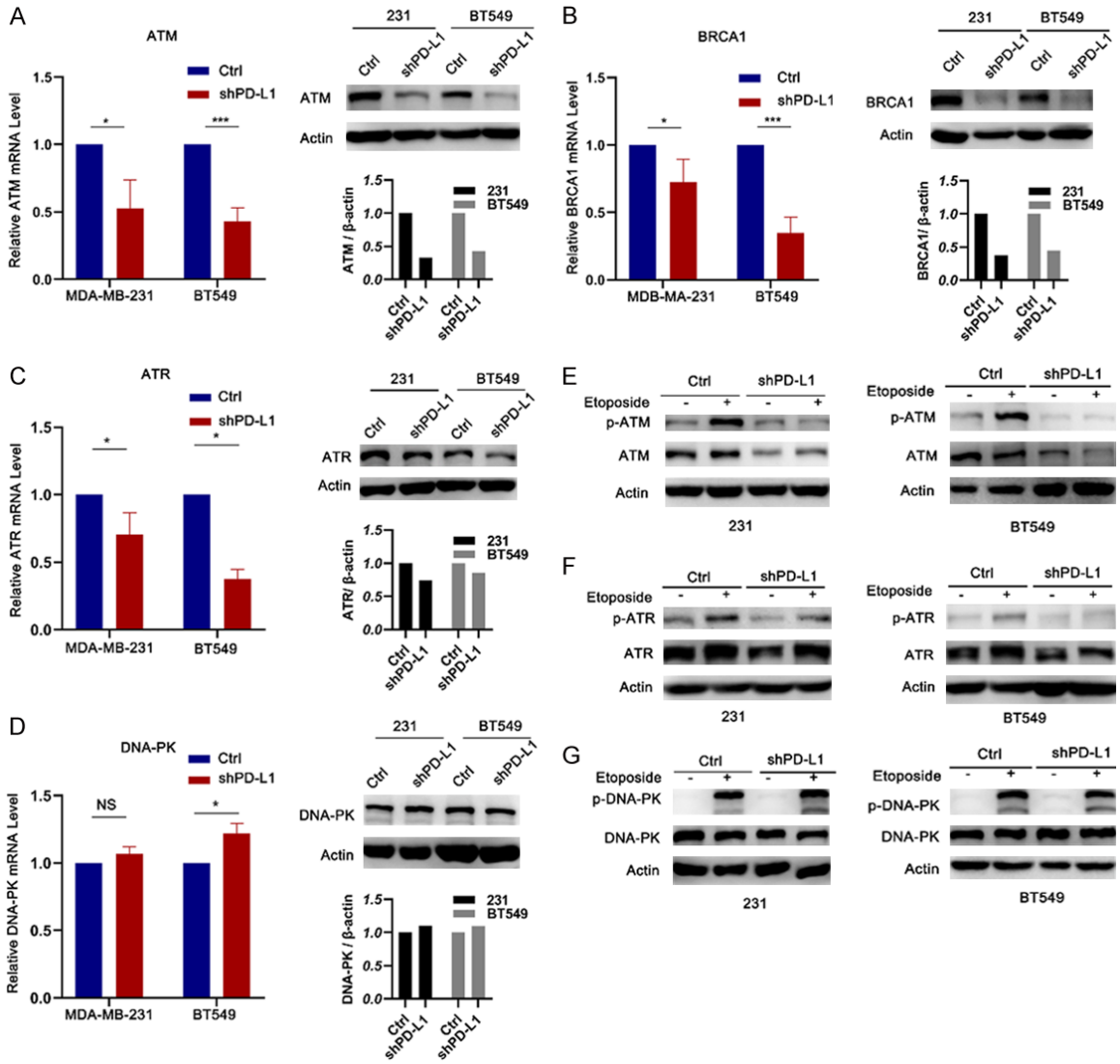

Figure 2. PD-L1 depletion leads to decreased expression and activation of ATM and ATR. A. QRT-PCR analysis and western blot analysis of ATM in MDA-MB-231 and BT549 PD-L1 WT and KD cells. B. QRT-PCR analysis and western blot analysis of BRCA1 in MDA-MB-231 and BT549 PD-L1 WT and KD cells. C. QRT-PCR analysis and western blot analysis of ATR in MDA-MB-231 and BT549 PD-L1 WT and KD cells. D. QRT-PCR analysis and western blot analysis of DNA-PK in MDA-MB-231 and BT549 PD-L1 WT and KD cells. E. Western blot analysis of the phosphorylation level of ATM (p-ATM S1981) in MDA-MB-231 and BT549 PD-L1 WT and KD cells treated with 50 μM etoposide for 20 h. F. Western blot analysis of the phosphorylation level of ATR (p-ATR Thr1989) in MDA-MB-231 and BT549 PD-L1 WT and KD cells treated with 50 μM etoposide for 20 h. G. Western blot analysis of the phosphorylation level of DNA-PK (p-DNA-PK S2056) in MDA-MB-231 and BT549 PD-L1 WT and KD cells treated with 50 μM etoposide for 20 h.

that ATM-mediated HR is compromised in these cells, which would render the cells highly dependent on DNA-PK-mediated NHEJ repair pathway and consequently more susceptible to DNA-PK inhibitor. To test our hypothesis, we treated the cells with NU7441, a specific small molecule inhibitor of DNA-PK, and evaluated their response by CCK-8 assay. We found that NU7441 inhibited the proliferation of PD-L1 KD cells more significantly than that of PD-L1 WT cells (**Figure 4A**), suggesting that PD-L1 depletion increased the sensitivity of cancer cells to DNA-PK inhibition. Similar results were observed by the crystal violet staining assay, as demonstrated by the higher inhibition of cell growth by NU7441 in PD-L1 KD cells (**Figures 4B** and S3A). In agreement, higher proportions of apoptotic cells were induced by NU7441 in

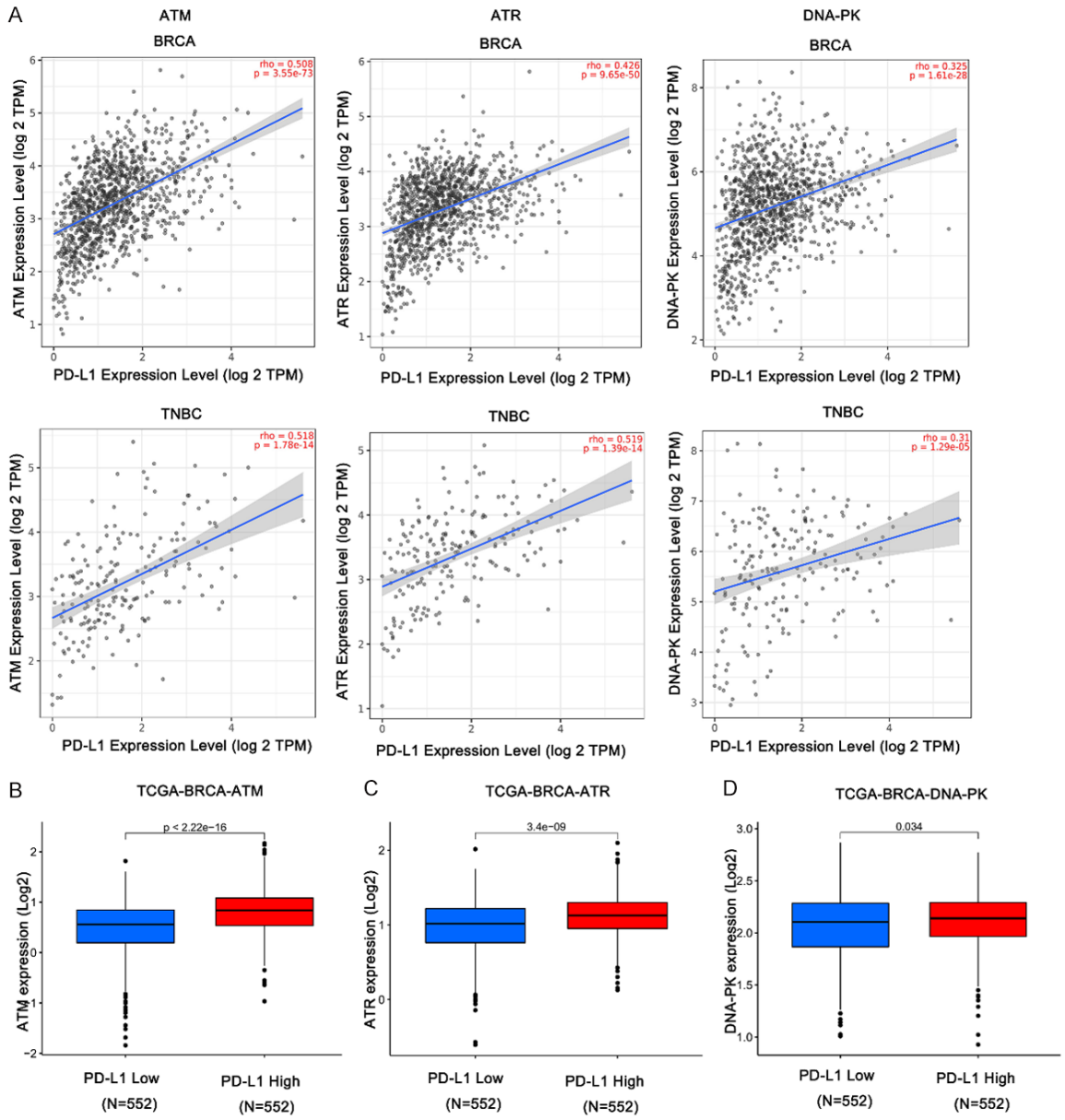

Figure 3. ATM expression is positively associated with PD-L1 expression in cancer patients. A. The correlations analysis of PD-L1 with ATM, ATR or DNA-PK in BRCA and TNBC patients was carried out by TIMER 2.0. B. The expression of ATM in BRCA with low or high PD-L1 expression was analyzed from TCGA database. C. The expression of ATR in BRCA with low or high PD-L1 expression was analyzed from TCGA database. D. The expression of DNA-PK in BRCA with low or high PD-L1 expression was analyzed from TCGA database.

PD-L1 depleted cells, as determined by flow cytometric analysis of 7-AAD staining (Figure S3B). Consistently, PD-L1 deficiency also conferred sensitivity to PI-103 (**Figure 4C**), another inhibitor of DNA-PK. In addition, PD-L1 depleted cells exhibited higher sensitivity to conventional DNA-damaging agents, such as etoposide (**Figure 4D**), cisplatin (**Figure 4E**), and their combination with NU7441, respectively (**Figure 4F**), but not to other DDR inhibitors, such as ATM inhibitor (KU60019), ATR inhibitor (VE-822), or PARP inhibitor (Olaparib) (Figure S3C-E). To further validate our findings, we assessed the levels of cleaved PARP and Caspase-3, two well-established markers for apoptosis. We found that upon treatment with NU7441, etoposide or their combination, PD-L1 KD cells showed higher levels of cleaved PARP and

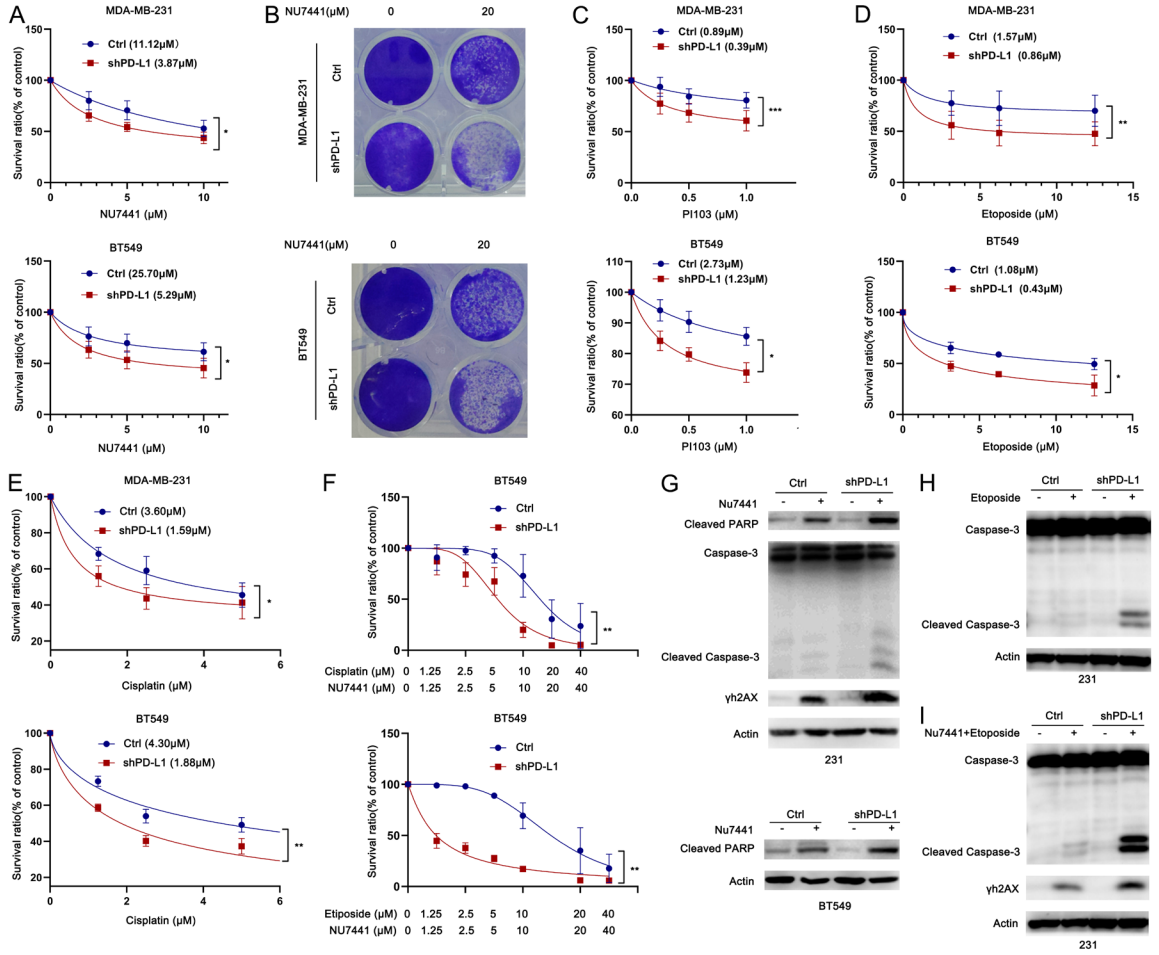

Figure 4. PD-L1 depletion confers sensitivity to DNA-PK inhibition and chemotherapy agents. A. Evaluation of cell proliferation by CCK8 assay in MDA-MB-231 and BT549 PD-L1 WT and KD cells treated with NU7441 for 48 h. B. Crystal violet staining of MDA-MB-231 and BT549 PD-L1 WT and KD cells after treatment with 20 μM NU7441 for 48 h. C. Evaluation of cell proliferation by CCK8 assay in MDA-MB-231 and BT549 PD-L1 WT and KD cells treated with PI103 for 48 h. D. Evaluation of cell proliferation by CCK8 assay in MDA-MB-231 and BT549 PD-L1 WT and KD cells treated with etoposide for 48 h. E. Evaluation of cell proliferation by CCK8 assay in MDA-MB-231 and BT549 PD-L1 WT and KD cells treated with cisplatin for 48 h. F. Evaluation of cell proliferation by CCK8 assay in BT549 PD-L1 WT and KD cells treated with NU7441 in combination with cisplatin or etoposide for 48 h. G. Western blot analysis of Caspase-3, cleaved PARP, and γH2AX in MDA-MB-231 and BT549 PD-L1 WT and KD cells treated with 30 μM NU7441 for 24 h. H. Western blot analysis of Caspase-3 in MDA-MB-231 PD-L1 WT and KD cells treated with 10 μM etoposide for 48 h. I. Western blot analysis of Caspase-3 and γH2AX in MDA-MB-231 PD-L1 WT and KD cells treated with the combination of NU7441 (5 μM) and etoposide (5 μM) for 48 h. The IC50 for each cell line is indicated in parentheses. All data are presented as the mean ± SD from at least three independent experiments.

Caspase-3, and increased DNA damage, as demonstrated by higher rH2AX levels (**Figures 4G-I**, S3F and S3G). Together, these results demonstrate that PD-L1 depletion sensitizes cancer cells to DNA-PK inhibition and conventional chemotherapy agents.

PD-L1 deficiency potentiates DNA damage-induced cGAS-STING signaling

Since PD-L1 deficiency impairs the repair of DNA damage, we reasoned that knockdown of PD-L1 may enhance DNA-damage induced cGAS-STING pathway. Indeed, compared with its WT counterpart, we found that PD-L1 depletion led to higher expression of cGAS, and increased phosphorylation of STING and TBK-1 in 231 cells upon Nu7441 or etoposide treatment (**Figure 5A** and **5B**). Conversely, overexpression (OE) of PD-L1 in A549 cells attenuated GAS-STING-TBK1 activation in response to etoposide (**Figure 5C**). In addition, q-RT-PCR analysis showed that PD-L1 depletion signifi-

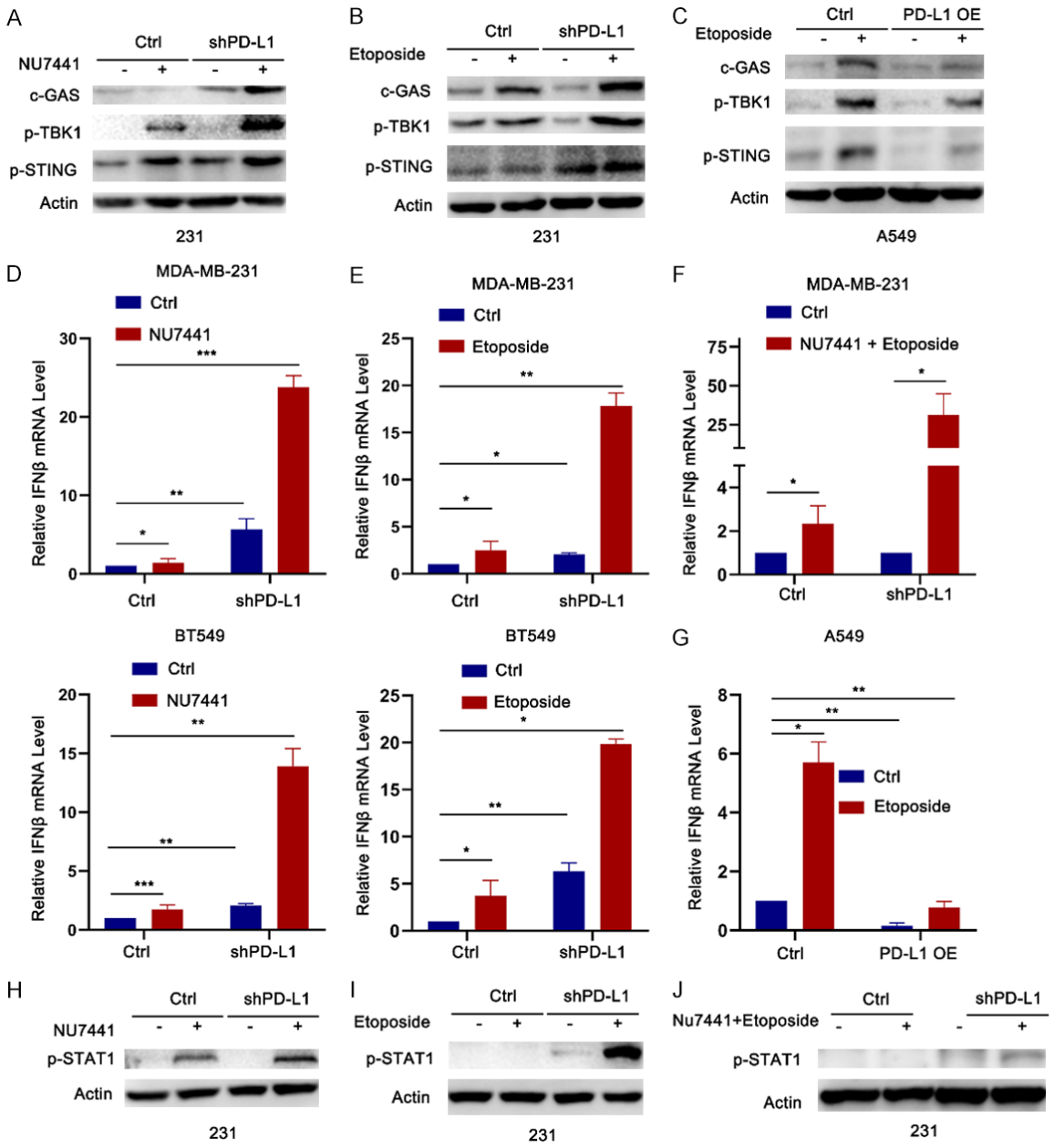

Figure 5. PD-L1 deletion enhances DNA damage-induced cGAS-STING signaling and IFNβ expression. A. Western blot analysis of cGAS, p-TBK1, and p-STING in MDA-MB-231 PD-L1 WT and KD cells treated with 20 μM NU7441 for 20 h. B. Western blot analysis of cGAS, p-TBK1, and p-STING in MDA-MB-231 PD-L1 WT and KD cells treated with 50 μM etoposide for 20 h. C. Western blot analysis of cGAS, p-TBK1, and p-STING in A549 PD-L1 WT and OE cells treated with 50 μM etoposide for 20 h. D. qRT-PCR analysis of IFNβ in MDA-MB-231 or BT549 PD-L1 WT and KD cells treated with 20 μM NU7441 for 20 h. E. qRT-PCR analysis of IFNβ in MDA-MB-231 or BT549 PD-L1 WT and KD cells treated with 50 μM etoposide for 20 h. F. QRT-PCR analysis of IFNβ in MDA-MB-231 or BT549 PD-L1 WT and KD cells treated with the combination of NU7441 (5 μM) and etoposide (5 μM) for 48 h. G. qRT-PCR analysis of IFNβ in A549 PD-L1 WT and OE cells treated with 50 μM etoposide for 20 h. H. Western blot analysis of p-STAT1 in MDA-MB-231 PD-L1WT and KD cells treated with 20 μM NU7441 for 20 h. I. Western blot analysis of p-STAT1 in MDA-MB-231 PD-L1 WT and KD cells treated with 50 μM etoposide for 20 h. J. Western blot analysis of p-STAT1 in MDA-MB-231 PD-L1 WT and KD cells treated with treated with the combination of NU7441 (5 μM) and etoposide (5 μM) for 48 h.

cantly increased the expression of IFNβ induced by Nu7441, etoposide or their combination in 231 and BT549 cells (**Figure 5D-F**), and PD-L1 OE in A549 cells led to a decrease in the

induction of IFNβ mRNA in response to the drug treatment (**Figures 5G**, S4A). The effect of PD-L1 KD or OE on IFNγ expression in response to DNA damage was similar to that of IFNβ but in a less significant extent (Figure S4B-D). Furthermore, knockdown PD-L1 triggered a more robust activation of IFN signaling upon treatment with Nu7441, etoposide or their combination, as evidenced by the increased phosphorylation of STAT1 (**Figures 5H-J**, S4E). Consistently, the level of phosphorylated STAT1 was decreased after PD-L1 OE (Figure S4F). Taken together, these results indicate PD-L1 deficiency enhances DNA damage-induced innate immunity.

Discussion

PD-L1 is a well-established immune checkpoint that is expressed on cancer cells and binds to PD-1 receptor on CD8+ T cells to inhibits their cytotoxic activity [22, 23]. However, accumulating evidence indicates that PD-L1 participates in a variety of cellular processes, such as sister chromatid separation, pyroptosis etc. [13-15, 17, 24], in addition to inhibiting T cell immune function. In this study, we reported that cancer cell-intrinsic PD-L1 was essential for DNA damage repair, potentially via regulating the HR repair pathway. By using the comet assay, we demonstrated that PD-L1 depleted cells exhibited deficiency in DNA repair capacity. Mechanically, we showed that the expression of ATM and BRCA1, the key molecules in HR repair pathway was significantly decreased upon PD-L1 depletion. Consistently, the activation of ATM in response to DNA damage was also dramatically attenuated in PD-L1 KD cells. These results suggest that PD-L1 is critical for the expression and activation of the critical molecules in HR pathway, and thus plays an important role in DNA damage repair. In good line with our results, PD-L1 has been shown to bind and stabilize the RNA of DNA damage-related genes [16]. Therefore, our findings, together with others' work, highlight the role of intracellular PD-L1 in DDR, especially in the HR pathway, thus broadening the understanding of PD-L1 biological functions.

Loss of certain elements of one DNA repair pathway can lead to dependence on a compensatory pathway [25]. Exploiting the dependence and targeting compensatory pathway is the basis of the principle of synthetic lethality, as exemplified by exquisite susceptibility of BRCA-deficient tumors to PARP inhibition [26]. In this study, we demonstrated a novel synthetic lethal interaction between PD-L1 and DNA-PK. We found that depletion of PD-L1 conferred sensitivity to DNA-PK inhibiton in TNBC, a highly aggressive cancer type with limited effective targeted therapies [27]. These results suggests that PD-L1 depleted cells with defect in ATM activation might be highly dependent on DNA-PK-mediated NHEJ repair pathway. Therefore, targeting this reliance would lead to the accumulation of DNA repair defects and consequent cell death. Further investigations are warranted to confirm the anti-tumor effect in vivo by genetic or pharmacological inhibition of intracellular PD-L1 in combination with the DNA-PK inhibitor. Consistent with our findings, the synthetic lethality between ATM and DNA-PK has been reported in a variety of tumors. The survival of ATM-deficient cancer cells highly depends on functional DNA-PK signaling, and DNA-PK inhibitors exhibit efficacy in ATM-deficient tumors [28-30]. Intriguingly, we did not find an increased sensitivity to PARP inhibition in PD-L1 depleted tumors, although the expression of BRCA1 was significantly downregulated in PD-L1 KD cells. The underlying molecular mechanisms remain to be further dissected.

Although PD-1/PD-L1 blockade immunotherapies have achieved notable clinical outcomes, only a small subset of cancer patients responds [27]. Emerging evidence suggests that the benefits of PD-1/PD-L1 inhibitors are highly dependent on the inflamed "hot" tumors which exhibit large amount of T cell infiltration and cytokines, such as IFNs [31]. Strategies are therefore needed to turn the non-responsive, "cold" tumors to responsive, "hot" tumors, to enhance the efficacy of existing immunotherapies. cGAS-STING agonists, which induce innate immune response and promote the priming and recruitment of tumor-specific CD8+ T cells, have been gaining increasing attentions recently [11]. Consistent with previous findings [32, 33], we demonstrated that DNA damaging-agents, such as etoposide and DNA-PK inhibitor, could slightly induce cGAS-STING signaling and IFNβ expression. Interestingly, we found that this signaling pathway and IFNβ induction was significantly enhanced after de-

pletion of intracellular PD-L1. Therefore, our findings unveil a novel link between tumor-intrinsic PD-L1 and innate immunity, suggesting that PD-1 not only protects tumors from T cell cytotoxicity, but could also act to inhibit innate immune pathways. The work provides a rationale for targeting intracellular PD-L1 combined with DNA damaging-agents to control tumors through promoting innate immunity, in addition to direct antitumor effects via synthetic lethality. Currently, a number of DNA-PK inhibitors (M9831, M3814 and CC115) have been evaluated in clinical trials, as monotherapy or combined with anti-PD-L1 antibody or DNA-damaging therapies in patients with advanced solid tumors [34, 35]. The combination of a DNA-PK inhibitor and anti-PD-L1 antibody has recently been shown to synergically inhibit tumor growth in a mouse model of colon cancer [36]. Based on our findings, we speculate that a more potent anti-tumor effect could be produced if the DNA-PK inhibitor is combined with an agent that reduces intracellular PD-L1 levels, in addition to blocking PD-L1/PD-1 binding. Therefore, our study suggests that intracellular PD-L1 represents a rational therapeutic target to enhance the efficacy of DDR inhibitors, and highlights the need for development of novel PD-L1 inhibitors that could suppress intracellular PD-L1 levels [37].

In conclusion, our study demonstrates the important role of PD-L1 in DNA repair, reveal the synthetic lethality between PD-L1 and DNA-PK, and connects PD-L1 with cGAS-STING mediated innate immunity. These findings shed new light on the understanding of PD-L1 biological functions and highlight targeting tumor-intrinsic PD-L1 as a novel strategy to increase tumoral IFN signaling to promote antitumoral immunity.

Acknowledgements

This work was funded by the following: National Natural Science Foundation of China (82172687 and 81972186 to LLS, 81572268 to DSZ); Natural Science Foundation of Tianjin (20JCYBJC25200 to LLS); Health Commission of Tianjin (TJWJ2021MS002 to L.S); Tianjin Key Medical Discipline (Specialty) Construction Project.

Disclosure of conflict of interest

None.

Address correspondence to: Linlin Sun, Tianjin Key Laboratory of Lung Cancer Metastasis and Tumor Microenvironment, Lung Cancer Institute, Tianjin Medical University General Hospital, Anshan Road 154, Heping District, Tianjin 300052, P. R. China. Tel: +22 60362409; Fax: +22 60362306; E-mail: lsun1@tmu.edu.cn; Diansheng Zhong, Department of Medical Oncology, Tianjin Medical University General Hospital, Anshan Road 154, Heping District, Tianjin 300052, P. R. China. Tel: +22 60817009; Fax: +22 60817009; E-mail: dzhong@tmu.edu.cn

References

[1] Hanahan D and Weinberg RA. Hallmarks of cancer: the next generation. Cell 2011; 144: 646-674.
[2] Aparicio T, Baer R and Gautier J. DNA double-strand break repair pathway choice and cancer. DNA Repair (Amst) 2014; 19: 169-175.
[3] Brown JS, O'Carrigan B, Jackson SP and Yap TA. Targeting DNA repair in cancer: beyond PARP inhibitors. Cancer Discov 2017; 7: 20-37.
[4] Minchom A, Aversa C and Lopez J. Dancing with the DNA damage response: next-generation anti-cancer therapeutic strategies. Ther Adv Med Oncol 2018; 10: 175883591878-6658.
[5] Marechal A and Zou L. DNA damage sensing by the ATM and ATR kinases. Cold Spring Harb Perspect Biol 2013; 5: a012716.
[6] Morrison C, Sonoda E, Takao N, Shinohara A, Yamamoto K and Takeda S. The controlling role of ATM in homologous recombinational repair of DNA damage. EMBO J 2000; 19: 463-471.
[7] Pilie PG, Tang C, Mills GB and Yap TA. State-of-the-art strategies for targeting the DNA damage response in cancer. Nat Rev Clin Oncol 2019; 16: 81-104.
[8] Cleary JM, Aguirre AJ, Shapiro GI and D'Andrea AD. Biomarker-guided development of DNA repair inhibitors. Mol Cell 2020; 78: 1070-1085.
[9] Decout A, Katz JD, Venkatraman S and Ablasser A. The cGAS-STING pathway as a therapeutic target in inflammatory diseases. Nat Rev Immunol 2021; 21: 548-569.
[10] Kwon J and Bakhoum SF. The cytosolic DNA-sensing cGAS-STING pathway in cancer. Cancer Discov 2020; 10: 26-39.
[11] Reislander T, Groelly FJ and Tarsounas M. DNA damage and cancer immunotherapy: a STING in the tale. Mol Cell 2020; 80: 21-28.
[12] Freeman GJ, Long AJ, Iwai Y, Bourque K, Chernova T, Nishimura H, Fitz LJ, Malenkovich N, Okazaki T, Byrne MC, Horton HF, Fouser L, Carter L, Ling V, Bowman MR, Carreno BM, Collins M, Wood CR and Honjo T. Engagement of

the PD-1 immunoinhibitory receptor by a novel B7 family member leads to negative regulation of lymphocyte activation. J Exp Med 2000; 192: 1027-1034.
[13] Cheon H, Holvey-Bates EG, McGrail DJ and Stark GR. PD-L1 sustains chronic, cancer cell-intrinsic responses to type I interferon, enhancing resistance to DNA damage. Proc Natl Acad Sci U S A 2021; 118: e2112258118.
[14] Hou J, Zhao R, Xia W, Chang CW, You Y, Hsu JM, Nie L, Chen Y, Wang YC, Liu C, Wang WJ, Wu Y, Ke B, Hsu JL, Huang K, Ye Z, Yang Y, Xia X, Li Y, Li CW, Shao B, Tainer JA and Hung MC. PD-L1-mediated gasdermin C expression switches apoptosis to pyroptosis in cancer cells and facilitates tumour necrosis. Nat Cell Biol 2020; 22: 1264-1275.
[15] Kornepati AVR, Vadlamudi RK and Curiel TJ. Programmed death ligand 1 signals in cancer cells. Nat Rev Cancer 2022; 22: 174-189.
[16] Tu X, Qin B, Zhang Y, Zhang C, Kahila M, Nowsheen S, Yin P, Yuan J, Pei H, Li H, Yu J, Song Z, Zhou Q, Zhao F, Liu J, Zhang C, Dong H, Mutter RW and Lou Z. PD-L1 (B7-H1) competes with the RNA exosome to regulate the DNA damage response and can be targeted to sensitize to radiation or chemotherapy. Mol Cell 2019; 74: 1215-1226, e1214.
[17] Yu J, Qin B, Moyer AM, Nowsheen S, Tu X, Dong H, Boughey JC, Goetz MP, Weinshilboum R, Lou Z and Wang L. Regulation of sister chromatid cohesion by nuclear PD-L1. Cell Res 2020; 30: 590-601.
[18] Zhang W, Jin J, Wang Y, Fang L, Min L, Wang X, Ding L, Weng L, Xiao T, Zhou T and Wang P. PD-L1 regulates genomic stability via interaction with cohesin-SA1 in the nucleus. Signal Transduct Target Ther 2021; 6: 81.
[19] Sato H, Niimi A, Yasuhara T, Permata TBM, Hagiwara Y, Isono M, Nuryadi E, Sekine R, Oike T, Kakoti S, Yoshimoto Y, Held KD, Suzuki Y, Kono K, Miyagawa K, Nakano T and Shibata A. DNA double-strand break repair pathway regulates PD-L1 expression in cancer cells. Nat Commun 2017; 8: 1751.
[20] Sun LL, Yang RY, Li CW, Chen MK, Shao B, Hsu JM, Chan LC, Yang Y, Hsu JL, Lai YJ and Hung MC. Inhibition of ATR downregulates PD-L1 and sensitizes tumor cells to T cell-mediated killing. Am J Cancer Res 2018; 8: 1307-1316.
[21] Tang Z, Pilie PG, Geng C, Manyam GC, Yang G, Park S, Wang D, Peng S, Wu C, Peng G, Yap TA, Corn PG, Broom BM and Thompson TC. ATR inhibition induces CDK1-SPOP signaling and enhances anti-PD-L1 cytotoxicity in prostate cancer. Clin Cancer Res 2021; 27: 4898-4909.
[22] Han Y, Liu D and Li L. PD-1/PD-L1 pathway: current researches in cancer. Am J Cancer Res 2020; 10: 727-742.
[23] Ju X, Zhang H, Zhou Z and Wang Q. Regulation of PD-L1 expression in cancer and clinical implications in immunotherapy. Am J Cancer Res 2020; 10: 1-11.
[24] Xiong W, Gao Y, Wei W and Zhang J. Extracellular and nuclear PD-L1 in modulating cancer immunotherapy. Trends Cancer 2021; 7: 837-846.
[25] Kaelin WG Jr. The concept of synthetic lethality in the context of anticancer therapy. Nat Rev Cancer 2005; 5: 689-698.
[26] Lord CJ and Ashworth A. PARP inhibitors: synthetic lethality in the clinic. Science 2017; 355: 1152-1158.
[27] Ou-Yang F, Li CL, Chen CC, Shen YC, Moi SH, Luo CW, Xia WY, Wang YN, Lee HH, Wang LH, Wang SC, Pan MR, Hou MF and Hung MC. Deglycosylated membrane PD-L1 in tumor tissues as a biomarker for responsiveness to atezolizumab (Tecentriq) in advanced breast cancer patients. Am J Cancer Res 2022; 12: 123-137.
[28] Bolt J, Vo QN, Kim WJ, McWhorter AJ, Thomson J, Hagensee ME, Friedlander P, Brown KD and Gilbert J. The ATM/p53 pathway is commonly targeted for inactivation in squamous cell carcinoma of the head and neck (SCCHN) by multiple molecular mechanisms. Oral Oncol 2005; 41: 1013-1020.
[29] Callen E, Jankovic M, Wong N, Zha S, Chen HT, Difilippantonio S, Di Virgilio M, Heidkamp G, Alt FW, Nussenzweig A and Nussenzweig M. Essential role for DNA-PKcs in DNA double-strand break repair and apoptosis in ATM-deficient lymphocytes. Mol Cell 2009; 34: 285-297.
[30] Riabinska A, Daheim M, Herter-Sprie GS, Winkler J, Fritz C, Hallek M, Thomas RK, Kreuzer KA, Frenzel LP, Monfared P, Martins-Boucas J, Chen S and Reinhardt HC. Therapeutic targeting of a robust non-oncogene addiction to PRKDC in ATM-defective tumors. Sci Transl Med 2013; 5: 189ra178.
[31] Haanen J. Converting cold into hot tumors by combining immunotherapies. Cell 2017; 170: 1055-1056.
[32] Nakamura K, Karmokar A, Farrington PM, James NH, Ramos-Montoya A, Bickerton SJ, Hughes GD, Illidge TM, Cadogan EB, Davies BR, Dovedi SJ and Valge-Archer V. Inhibition of DNA-PK with AZD7648 sensitizes tumor cells to radiotherapy and induces type I IFN-dependent durable tumor control. Clin Cancer Res 2021; 27: 4353-4366.
[33] Brzostek-Racine S, Gordon C, Van Scoy S and Reich NC. The DNA damage response induces IFN. J Immunol 2011; 187: 5336-5345.
[34] Medova M, Medo M, Hovhannisyan L, Munoz-Maldonado C, Aebersold DM and Zimmer Y. DNA-PK in human malignant disorders: mech-

anisms and implications for pharmacological interventions. Pharmacol Ther 2020; 215: 107617.
[35] Sun W, Zhang Q, Wang R, Li Y, Sun Y and Yang L. Targeting DNA damage repair for immune checkpoint inhibition: mechanisms and potential clinical applications. Front Oncol 2021; 11: 648687.
[36] Tan KT, Yeh CN, Chang YC, Cheng JH, Fang WL, Yeh YC, Wang YC, Hsu DS, Wu CE, Lai JI, Chang PM, Chen MH, Lu ML, Chen SJ, Chao Y, Hsiao M and Chen MH. PRKDC: new biomarker and drug target for checkpoint blockade immunotherapy. J Immunother Cancer 2020; 8: e000485.
[37] Wu Q, Jiang L, Li SC, He QJ, Yang B and Cao J. Small molecule inhibitors targeting the PD-1/PD-L1 signaling pathway. Acta Pharmacol Sin 2021; 42: 1-9.

Table S1. Primers used are as follows

	Former primer	Reverse primer
Human PD-L1	5'GGACAAGCAGTGACCATCAAG3'	5'CCCAGAATTACCAAGTGAGTCCT3'
Human ATM	5'TTGATCTTGTGCCTTGGCTAC3'	5'TATGGTGTACGTTCCCCATGT3'
Human ATR	5'GGCCAAAGGCAGTTGTATTGA3'	5'GTGAGTACCCCAAAAATAGCAGG3'
Human DNA-PK	5'CTGTGCAACTTCACTAAGTCCA3'	5'CAATCTGAGGACGAATTGCCT3'
Human BRCA1	5'TTGTTACAAATCACCCCTCAAGG3'	5'CCCTGATACTTTTCTGGATGCC3'
Human IFNβ	GCTTGGATTCCTACAAAGAAGCA	ATAGATGGTCAATGCGGCGTC
Human IFNγ	TCGGTAACTGACTTGAATGTCCA	TCGCTTCCCTGTTTTAGCTGC
Human GAPDH	5'GGAGCGAGATCCCTCCAAAAT3'	5'GGCTGTTGTCATACTTCTCATGG3'

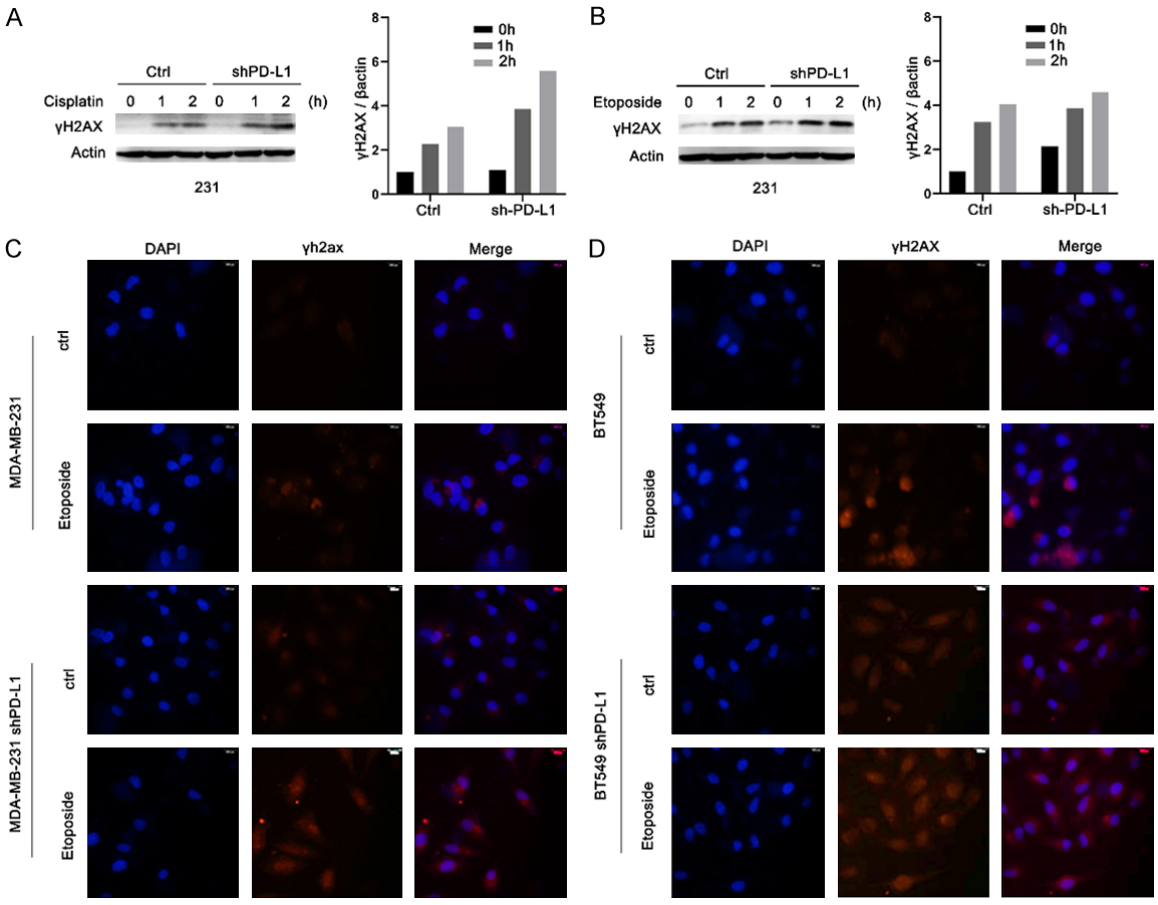

Figure S1. PD-L1 depletion leads to increased rH2AX in response to chemotherapy agents. A. Western blot analysis of γH2AX in MDA-MB-231 cells with or without PD-L1 KD treated with 10 μM cisplatin for indicated time. B. Western blot analysis of γH2AX in MDA-MB-231 cells with or without PD-L1 KD treated with 50 μM etoposide for indicated time. C. Immunofluorescence analysis of rH2AX in MDA-MB-231 PD-L1 WT and KD cells treated with etoposide 50 μM for 20 h. D. Immunofluorescence analysis of rH2AX in BT549 PD-L1 WT and KD cells treated with etoposide 50 μM for 20 h.

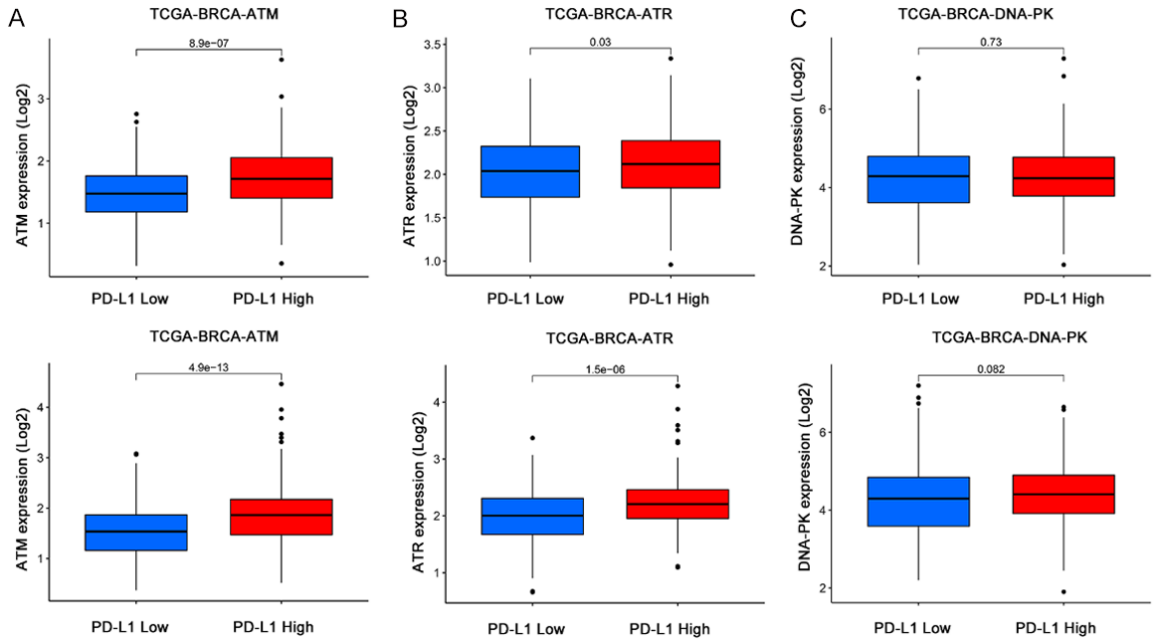

Figure S2. The correlation analysis of DDR genes with PD-L1 expression in BRCA patients with or without radiation therapy. A. The expression of ATM in BRCA patients' samples with low or high PD-L1 expression was analyzed from TCGA database. Upper panel: without radiation therapy, lower panel: with radiation therapy. B. The expression of ATR in BRCA patients' samples with low or high PD-L1 expression was analyzed from TCGA database. Upper panel: without radiation therapy, lower panel: with radiation therapy. C. The expression of DNA-PK in BRCA patients' samples with low or high PD-L1 expression was analyzed from TCGA database. Upper panel: without radiation therapy, lower panel: with radiation therapy.

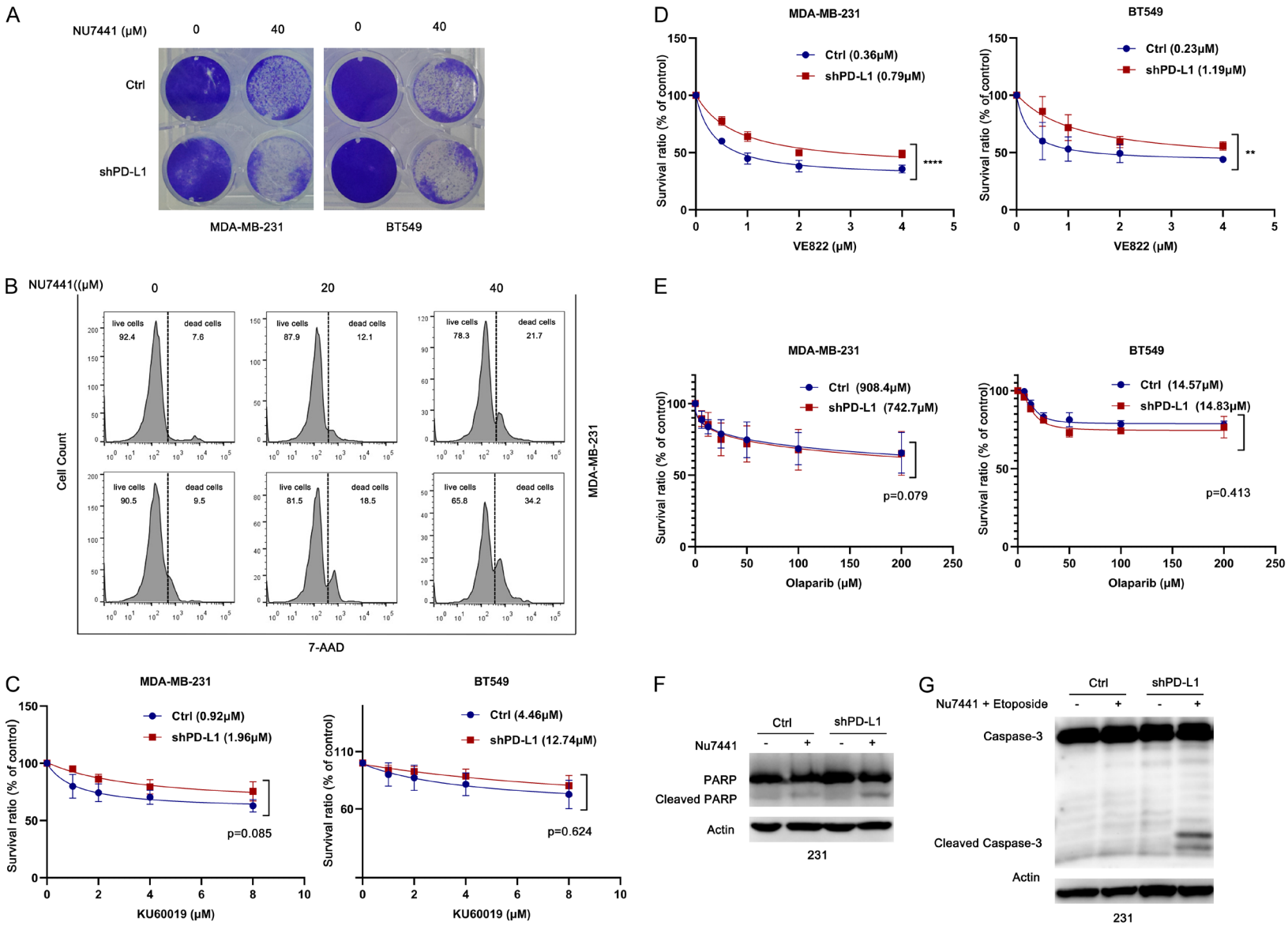

Figure S3. The effect of PD-L1 depletion on the sensitivity of cancer cells to DDR inhibitors. A. Crystal violet staining of MDA-MB-231 and BT549 PD-L1 WT and KD cells after treatment with 40 μM NU7441 for 48 h. B. Flow cytometric analysis of apoptosis in MDA-MB-231 PD-L1 WT and KD cells after treatment with NU7441 at the indicated dose for 48 h. C. Evaluation of cell proliferation by CCK8 assay in MDA-MB-231 and BT549 PD-L1 WT and KD cells treated with ATM inhibitor KU60019.

D. Evaluation of cell proliferation by CCK8 assay in MDA-MB-231 and BT549 PD-L1 WT and KD cells treated with ATR inhibitor VE-822. E. Evaluation of cell proliferation by CCK8 assay in MDA-MB-231 and BT549 PD-L1 WT and KD cells treated with PARP inhibitor Olaparib. F. Western blot analysis of PARP in MDA-MB-231 PD-L1 WT and KD cells treated with NU7441 (30 μM) for 24 h. G. Western blot analysis of Caspase-3 in MDA-MB-231 PD-L1 WT and KD cells treated with the combination of NU7441 (2.5 μM) and etoposide (2.5 μM) for 48 h. The IC50 for each cell line is indicated in parentheses. All data are presented as the mean ± SD from at least three independent experiments.

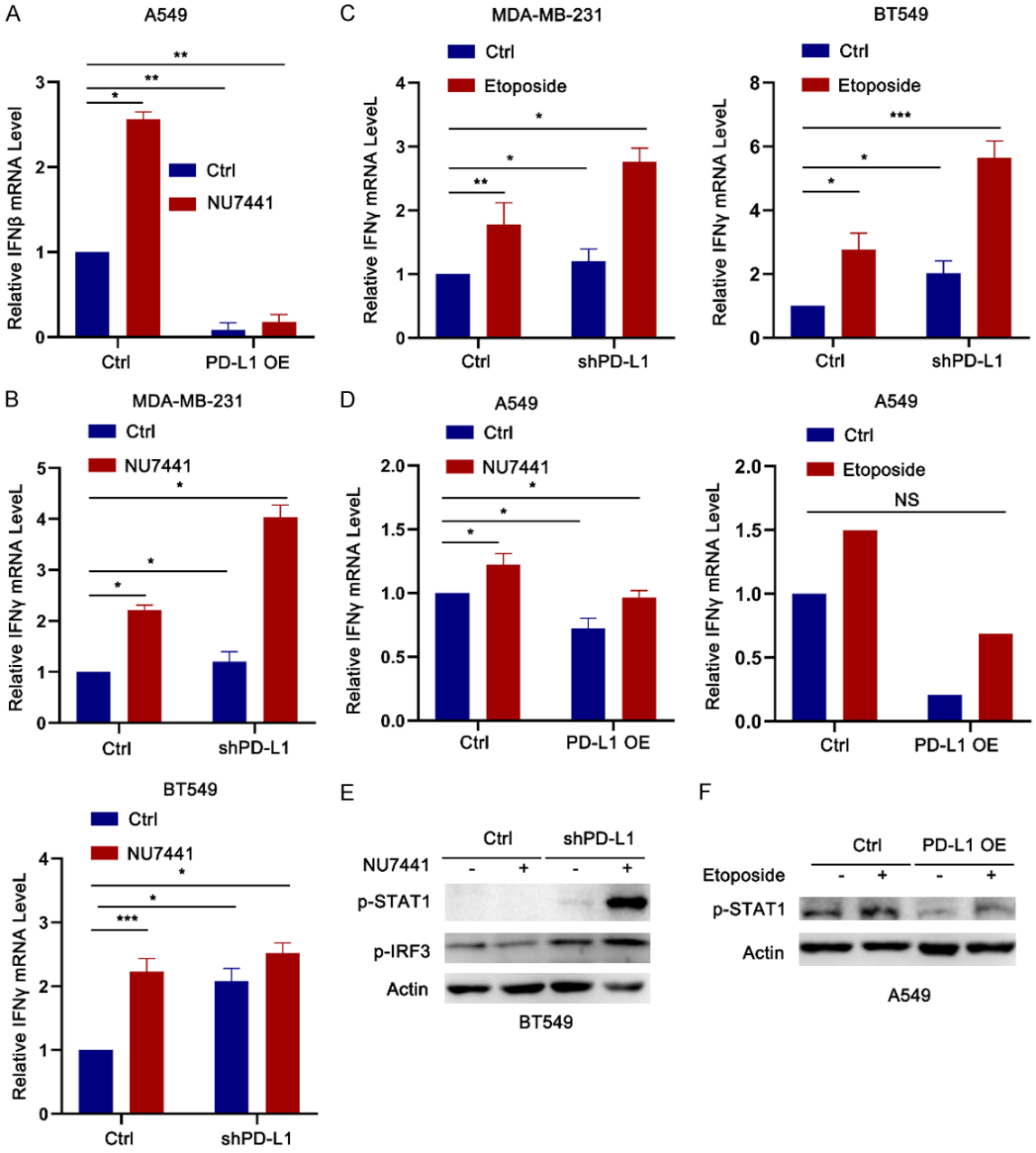

Figure S4. PD-L1 regulates the induction of IFNβ and IFNγ and STAT1 phosphorylation in response to DNA damage. A. QRT-PCR analysis of IFNβ in A549 PD-L1 WT and OE cells treated with 20 μM NU7441 for 20 h. B. QRT-PCR analysis of IFNγ in MDA-MB-231 and BT549 PD-L1 WT and KD cells treated with 20 μM NU7441 for 20 h. C. qRT-PCR analysis of IFNγ in MDA-MB-231 and BT549 PD-L1 WT and KD cells treated with 50 μM etoposide for 20 h. D. QRT-PCR analysis of IFNγ in A549 PD-L1 WT and OE cells treated with 50 μM etoposide for 20 h. E. Western blot analysis of p-STAT1 in BT549 PD-L1 WT and KD cells treated with 20 μM NU7441 for 20 h. F. Western blot analysis of p-STAT1 in A549 PD-L1 WT and OE cells treated with 50 μM etoposide for 20 h.